Journal of the Australian Ceramic Society (2022) 58:1433–1443
https://doi.org/10.1007/s41779-022-00779-2

RESEARCH

An investigation on the thermal and microstructural properties of low-cost pressureless sintered silicon nitride (Si_3N_4) ceramics incorporated with Y_2O_3-SiO_2-MgO

Pınar Uyan[1,2] · Özgür Cengiz[3] · Servet Turan[4]

Received: 4 February 2022 / Revised: 18 June 2022 / Accepted: 26 June 2022 / Published online: 19 September 2022

Abstract

Y_2O_3-SiO_2-MgO-incorporated silicon nitride (Si_3N_4) ceramics were investigated systemically to obtain cost-effective production and the effect of sintering temperature on the microstructure and thermal properties was studied. An α-Si_3N_4 starting powder was used for preparing the samples and sintered under a pressure of one bar nitrogen gas pressure at 1650, 1700, 1750, 1800, and 1850 ℃ for 2 h. The crystallisation behaviour of the ceramics was promoted by sintering temperatures as evidenced by the XRD results. A different secondary phase, melilite ($Y_2Si_3O_3N_4$) formation, was detected using SEM micrographs of the final microstructures of the samples sintered at higher temperatures above 1700 ℃ which had a positive effect on thermal properties. The values of thermal conductivity increased by about 75.5% with increasing sintering temperature. The highest thermal conductivity (53.58 W/(mK)) was achieved with the highest sintering temperature of 1850 ℃. The results revealed that ternary sintering additives, such as Y_2O_3-SiO_2-MgO, had a potential for low-cost production of Si_3N_4 ceramics with enhanced thermal properties.

Keywords Silicon nitride · Pressureless sintering · Thermal properties · Microstructure-final · Ternary sintering additives

Introduction

Silicon nitride (Si_3N_4) ceramics are currently being used as substrates in power electronic devices for more than three decades [1–3]. In the non-metallic single crystals such as SiC (silicon carbide), AlN (aluminium nitride), and BP, the conductivity values are above 300 W/(mK) [4] and that SiC and AlN ceramics are produced with thermal conductivity above 200 W/(mK) [5]. However, their reliability is low due to their low mechanical properties. In addition to that, the use of SiC ceramics is limited because of their high dielectric constant and low electrical resistance [5]. It is known that the theoretical thermal conductivity of β-Si_3N_4 crystals is 200 W/(mK) or higher [3] and determined thermal conductivity of β-Si_3N_4 at room temperature is 200–320 W/(mK) [6]. Silicon nitride (Si_3N_4) ceramics are, thus, essential components for high performance substrates in electronic devices.

Several research workers have investigated the general implementations of Si_3N_4 ceramics. Nevertheless, high production cost still has been a challenging issue. Therefore, lowering the production cost of Si_3N_4 ceramics is precisely the purpose of this study. A search of the literature revealed only a few studies on this purpose corresponding to facilitate production ability and decrement of fabrication costs. Many production methods have been used for the production of Si_3N_4 ceramics. Current methods employed in the production of Si_3N_4 ceramics with excellent performance at the required parameters, high temperatures (1900–1950 ℃) with high nitrogen gas pressures (5–100 bar), and long annealing times (4–12 h), were reported [6–8]. In order to obtain high thermal conductivity at lower sintering temperatures, densification requires to be accomplished. For this, the particle size of the starting powder should be reduced, resulting

✉ Pınar Uyan
pinar.uyan@bilecik.edu.tr

1 Metallurgy Programme, Vocational School, Bilecik Seyh Edebali University, 11210 Bilecik, Turkey

2 Biotechnology Application and Research Centre, Bilecik Seyh Edebali University, 11230 Bilecik, Turkey

3 Department of Ceramic, Afyon Kocatepe University, 03100 Afyonkarahisar, Turkey

4 Department of Materials Science and Engineering, Eskisehir Technical University, 26480 Eskisehir, Turkey

from the use of fine-grained powder that makes sintering easier [9]. It is possible to increase the density of Si_3N_4 by using different techniques such as gas pressure sintering (GPS), hot isotropic pressing (HIP), and pressureless sintering (PS) [9]. By using the GPS method, higher densities can be obtained by reducing the amount of the additive raw powder at higher temperatures [10–13]. The HIP and GPS methods are costly due to the difficulties faced during production and industrial use is limited in the HIP method [14]. Until recently, the highest thermal conductivity achieved was 177 W/(mK) in a silicon nitride ceramic produced using the reaction-bonded sintering method (SRBSN) [5]. PS has both lower cost and is easier method for Si_3N_4 ceramic production in comparison to other methods.

The identified production parameters affecting the final conductivity are grain size, grain size distribution, grain boundary films, lattice defects, secondary boundary phase formation, and crystallisation [15, 16]. Thus, in order to obtain high densification, utilisation of suitable starting powder and incorporation of sintering additions on the composition are the key factors. In recent studies, Si_3N_4 ceramics requiring high-temperature sintering with thermal conductivity between 50 and 177 W/(mK) were produced using a suitable starting powder and sintering additions, e.g., lithia, magnesia, ceria, or cordierite [6, 8, 9, 14]. A widely varying effects were achieved by using ternary additives, including metal oxides such as TiO_2, MgO, ZrO_2, Y_2O_3, Yb_2O_3, Al_2O_3, La_2O_3, and Sc_2O_3 [16–18] for the densification. To promote liquid-phase sintering associated with α-phase, rare earth oxides and transition metal oxides have been widely employed as sintering aids. In addition, the increment in the radius of the rare earth ion is directly proportional to the increment in activation energy required for the α to β-Si_3N_4 phase transformation, and this reaction plays a significant role in improving thermal conductivity. Hence, Y_2O_3 is the most selected oxide for the use as a sintering additive owing to its high electropositivity and ionic valency of 3 + [19–21]. Gas pressure sintering (GPS) method was already used for the production of Y_2O_3-doped Si_3N_4 ceramic compositions and the values of thermal diffusivity due to different cooling cycles were investigated [22]. Several sintering additives Y_2O_3–MgO, Y_2O3–MgF_2, YF_3–MgO, and YF_3–MgF_2 were also used in the production of Si_3N_4 ceramics by GPS [23]. Until recently, a search of the literature revealed only a few studies on cost-effective production Si_3N_4 ceramics. Therefore, the aim of this investigation was to lower the cost and energy consumption of the studied Si_3N_4 ceramic production with developed thermal properties by lowering temperature and soaking time. Recent studies indicated that the thermal transport values of ceramics are affected by the oxygen on their surface and sintering agents such as MgO, Y_2O_3 and Al_2O_3 [24, 25]. Therefore, MgO was selected as a metal oxide additive with Y_2O_3 as a rare earth oxide additive in this study to obtain high thermal conductivity as well as high density. Previous investigations have shown that thermal conductivity can be improved by forming compounds, e.g., $Y_2Si_3O_3N_4$, as a result of the reaction of rare earth oxides with Si_3N_4 and SiO_2 [19, 26]. For this reason, SiO_2 was selected as a densifying additive due to its refractoriness and was incorporated in the compositions in this study. Considering the potential effects of Y_2O_3 and MgO with SiO_2 on Si_3N_4 ceramics has not been discussed in recent investigations; this study was conducted with the purpose of evaluating the effect of Y_2O_3-MgO-SiO_2 ternary sintering additives on crystallisation and the thermal properties of silicon nitrides produced by PS (pressureless sintering) technique which leads to cost reduction. For this purpose, the samples incorporated with the selected ternary additives (Y_2O_3-MgO-SiO_2) were prepared by subjecting α-Si_3N_4 powder to PS at relatively lower temperatures of 1650, 1700, 1750, 1800, and 1850 ℃, under one bar nitrogen gas pressure for 2 h. Thermal diffusivity was measured to determine the thermal properties. X-ray diffraction (XRD) and scanning electron microscopy (SEM) fitted with EDX were used to identify the phase formation and its effect on thermal properties. Consequently, the compositions incorporated with these sintering additions produced by PS and the effects of temperature, soaking time, and sintering additives on the microstructure and final properties have been further discussed.

Experimental

The sintering processes was performed on a sample prepared by using MgO (purity 99.9%, Sigma Aldrich Merck KGaA, USA), Y_2O_3 (purity 99.9%, Sigma-Aldrich Merck KGaA, USA) and SiO_2 (purity 99.9%, Sigma Aldrich Merck KGaA, USA) oxide additives (MgO:Y_2O_3:SiO_2; 2:1:2, in molar ratio) for the formation of a highly dense structure with high thermal conductivity with the use of α-Si_3N_4 (UBE Industries Co., Japan) starting powder (2% β phase, particle size ~ 0.5 µm, 1.4 O%). After mixing of all the powders and milling in alcohol for 1.5 h at 300 rpm in a planetary ball mill (Fritsch-Pulverisette 5, Germany), the slurries were dried with a rotary-evaporator (Heidolph 4001, Germany). An initial uniaxial pressure (Alfa model) of 25 MPa was applied to the powders to form a green compact, and then was cold isostatically pressed (CIP- model FPG2568/2569, Stansted Fluid Power, UK) under 300 MPa. The sintering process was performed via the PS (Thermal Technology-1000–4560-FP2000) furnace at the temperatures of 1650, 1700, 1750, 1800, and 1850 ℃ for 2 h under one bar nitrogen gas pressure. The rate of heating and cooling was 10 °C/min and 70 °C/min, respectively.

The bulk density values of the sintered pellets were determined using the Archimedes according to the

standard (ASTM-C373) methods. The X-ray diffractogram of the powders and the sintered pellets was recorded by XRD (Rigaku Rint 2000, Japan) equipped with Cu-Kα ($\lambda = 1.54056$ A°) radiation (working at 40 kV, scanning velocity of 1 °C/min) in order to identify phase content. Microstructural investigations were performed on powders using a Schottky field emission gun (S-FEG) scanning electron microscope (SEM Zeiss SUPRA 50 VP, Germany) and on bulk specimens using SEM (Zeiss SUPRA 40 VP-FEG, Germany) and energy dispersive X-ray spectrometer (EDX, Bruker Nano GmbH, Berlin, Germany).

The disk-like samples were prepared with a diameter of 12.7 mm and a thickness of 2.0 mm for thermal diffusivity measurements using a laser-flash device (Netzsch LFA-457, Germany). Each point in the thermal diffusivity graphics indicates average values of thermal diffusivity. A Cape-Lehman model was used for the calculations, which takes radial thermal losses into account. A heat capacity (Cp) of 0.7 J/g-K was used for all the samples in accordance with previous studies for Si_3N_4 ceramics [27].

Results and discussions

The XRD pattern of the Si_3N_4 starting powder is shown in Fig. 1. The initial powder consists of two phases of silicon nitride as substantiated by the identified major peaks of α-Si_3N_4 (silicon nitride-alpha) accompanied with minor peaks of β-Si_3N_4 (silicon nitride-beta). The approximate ratio of α-Si_3N_4 (silicon nitride-alpha) and β-Si_3N_4 (silicon nitride-beta) was calculated as 98% α and 2% β by using the intensities of the peaks obtained from the planes (102)-(210) and (101)-(210), respectively, which is revealed by the method proposed by Gazzara and Messier [28].

SEM images taken from the starting powder are shown in Fig. 2. Observations of the micrographs indicate that the starting particle size of the powder is very fine (on a nanometre scale).

Comparative X-ray patterns obtained from the surface of the sintered samples at various temperatures are given in Fig. 3. The major phase observed in all samples was β-Si_3N_4 (silicon nitride-beta, PDF 00–33-1160, hexagonal, P63/m [176]). $Y_2Si_3O_3N_4$ (melilite) phase (PDF

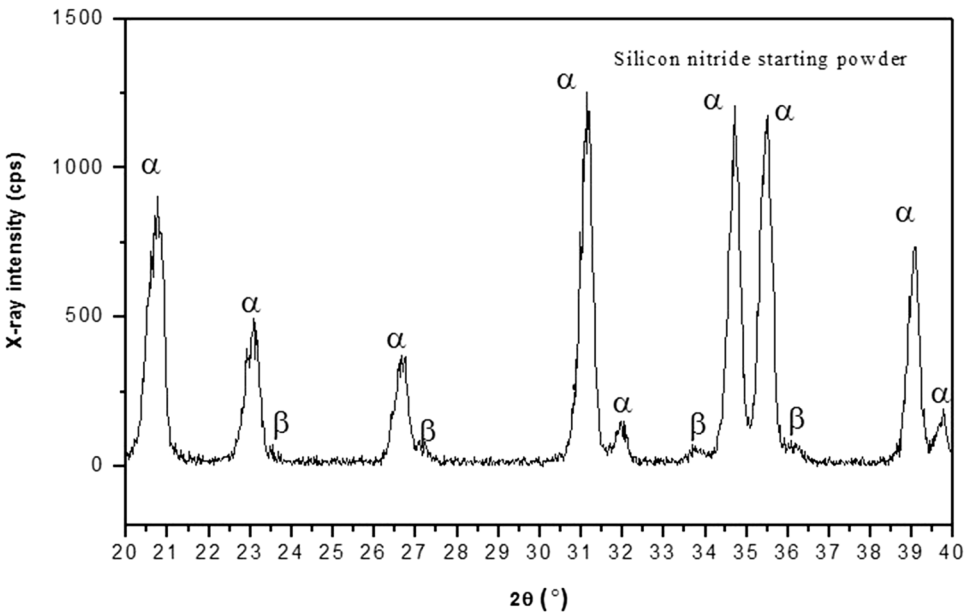

Fig. 1 XRD patterns of the Si_3N_4 starting powder

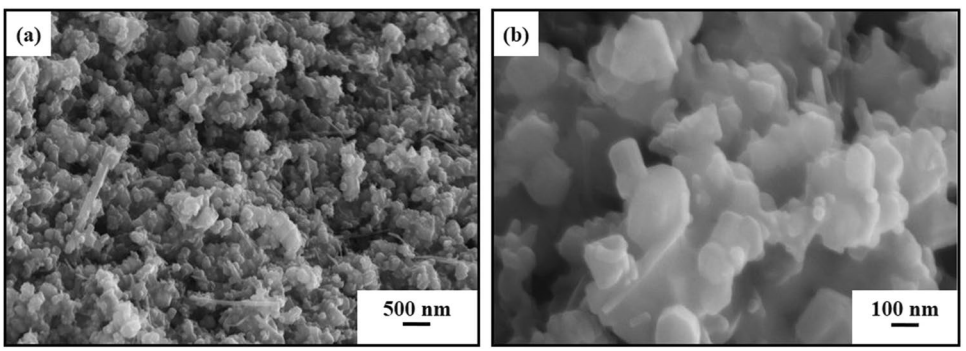

Fig. 2 Morphology of Si_3N_4 powders (**a**) 10 Kx and (**b**) 50 Kx

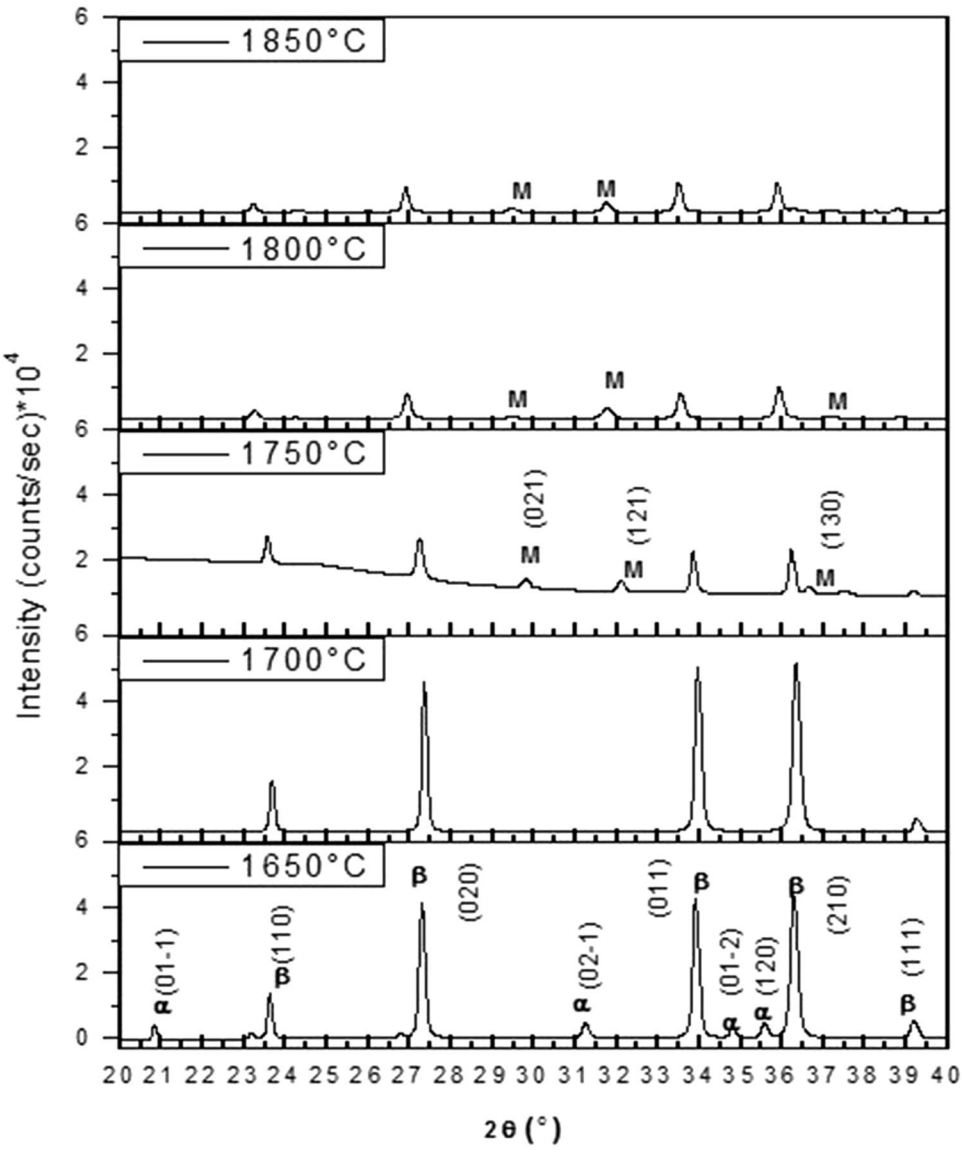

Fig. 3 X-ray patterns of sintered samples at various temperatures (M, melilite ($Y_2Si_3O_3N_4$); β, β-Si_3N_4 (Silicon nitride-beta))

00–76-0724, tetragonal, P-421 m [113]) was observed in the samples sintered at temperatures of 1750 °C, 1800 °C, and 1850 °C as the secondary phase. The secondary and minor phase, melilite formation, is consistent with the possible phases in the Si_3N_4-Y_2O_3-SiO_2 phase diagram [29]. Diffraction peaks of melilite (021) and (121) planes were detected at temperatures of 1750, 1800, and 1850 °C. Nevertheless, this phase was not detected at 1650 °C and 1700 °C. Thus, the higher sintering temperatures resulted in the formation of $Y_2Si_3O_3N_4$ phase suggesting that lower sintering temperatures were not enough for crystallisation from the liquid phase and therefore secondary crystalline phase ($Y_2Si_3O_3N_4$) formation. The highest peak intensity of the $Y_2Si_3O_3N_4$ phase was detected in the sample sintered at 1750 °C. The peak intensity of this phase was lower in the ceramics sintered at temperatures of 1800 °C and 1850 °C than the ceramics sintered at 1750 °C (Fig. 3) related to crystallisation of melilite ($Y_2Si_3O_3N_4$).

The full width at half maximum (FWHM) values of the peaks obtained from X-ray diffraction (Fig. 3) and thus the crystallite size of β-Si_3N_4 (Silicon nitride-beta) phase was calculated using the following Scherrer Eq. 1 [30].

$$D = \frac{K\lambda}{\beta cos\theta} \tag{1}$$

where D is the crystallite size; K is the Scherrer constant (typically equal to 0.9); λ is the X-ray wavelength ($CuK\alpha = 1.54056$ Å); β is the line broadening at FWHM in radians; and θ is the Bragg's angle in degrees which is half of 2θ value [30]. The major phase observed in all samples was β-Si_3N_4 (silicon nitride-beta, PDF 00–33-1160,

hexagonal, P63/m [176]) although the peak intensities were decreased with the increasing sintering temperatures (Fig. 3). The secondary phase formation was first detected at the sintering temperature of 1750 °C. Therefore, the mean of major and minor peaks of the major phase, β-Si_3N_4 (silicon nitride-beta), were selected at the sintering temperature of 1750 °C to calculate the average crystallite (particle) size. With reference to the Eq. 1, the average crystallite size value (D) of the β-Si_3N_4 (silicon nitride-beta) phase was calculated as 20.20 nm.

High-magnification SEM images of the samples are given in Fig. 4. It has been already known that the coarser grain size and wider grain size distribution were detected in the silicon nitride ceramic samples incorporated with Y_2O_3 [31]. It can therefore be stated that an increased grain size and rod-like grains led to reduced scattering effect which is advantageous in order to achieve enhanced thermal conductivity (Fig. 4). The images collected from the samples sintered at 1650 °C and 1700 °C indicated that the samples possess similar microstructures. It was observed that as the sintering temperature increased from 1650 to 1700 °C, a slight grain growth occurred (Fig. 4(a) and Fig. 4(c)). Besides, the thermal conductivity values were increased with the observed densities (Fig. 4 and Table 1). The revealed microstructures of the samples sintered at the temperatures up to 1750 ℃. It is seen that N-melilite ($R_2Si_3O_3N_4$) phase formation takes place indicating the presence of a secondary crystalline phase formed at 1750 ℃ as evidenced in XRD patterns (Fig. 2). The elemental analysis of the samples is reported in Fig. 5. Sintering at higher temperatures above 1600 ℃ might be expected to promote reactions occurred in Si_3N_4 ceramics as expressed in Eqs. (2) and (3) [29].

$$Si_3N_4 + 3SiO_2(l) = 6SiO(g) + 2N_2(g) \quad (2)$$

$$Si_3N_4 + SiO_2(s,l) = 2SiO(g) + 2Si(l) + 2N_2(g) \quad (3)$$

The reactions could proceed forward easily as a consequence of the lower nitrogen gas pressure. During the grain growth process of β-Si3N4, SiO2 involved in the liquid

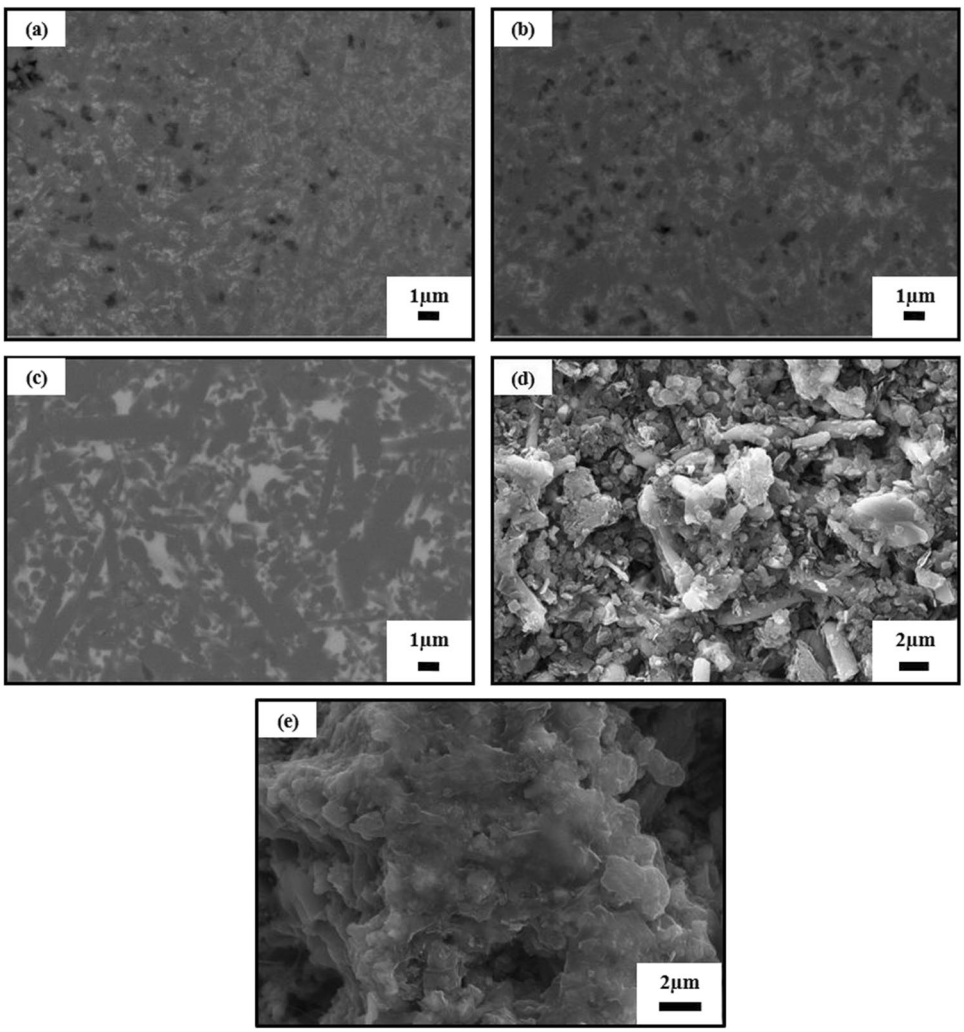

Fig. 4 Microstructure images of the samples sintered at (**a**) 1650 °C, (**b**) 1700 °C, (**c**) 1750 °C, (**d**) 1800 °C, and (**e**) 1850 ℃ temperatures

Table 1 Physical and thermal properties of the Si_3N_4 ceramics sintered at different sintering temperatures

Sintering temperature (°C)	Density (g/cm^3)	O.P[(a)] (%)	M.C[(b)] (%)	Secondary phases	Thermal diffusivity (RT [(c)]) (mm^2/s)	Thermal diffusivity (1000 °C) (mm^2/s)	Thermal conductivity (RT [(c)]) (W/(mK))	Thermal conductivity (1000 °C) (W/(mK))
1650	3.06	0.22	− 7.9	-	14.25	3.00	30.53	6.43
1700	3.07	0.22	− 8.3	-	15.38	4.17	33.05	8.96
1750	3.10	2.19	− 10.2	M	22.24	4.50	48.26	9.77
1800	3.11	2.26	− 10.5	M	23.72	4.51	51.64	9.82
1850	3.15	0.73	− 11.1	M	24.30	5.09	53.58	11.22

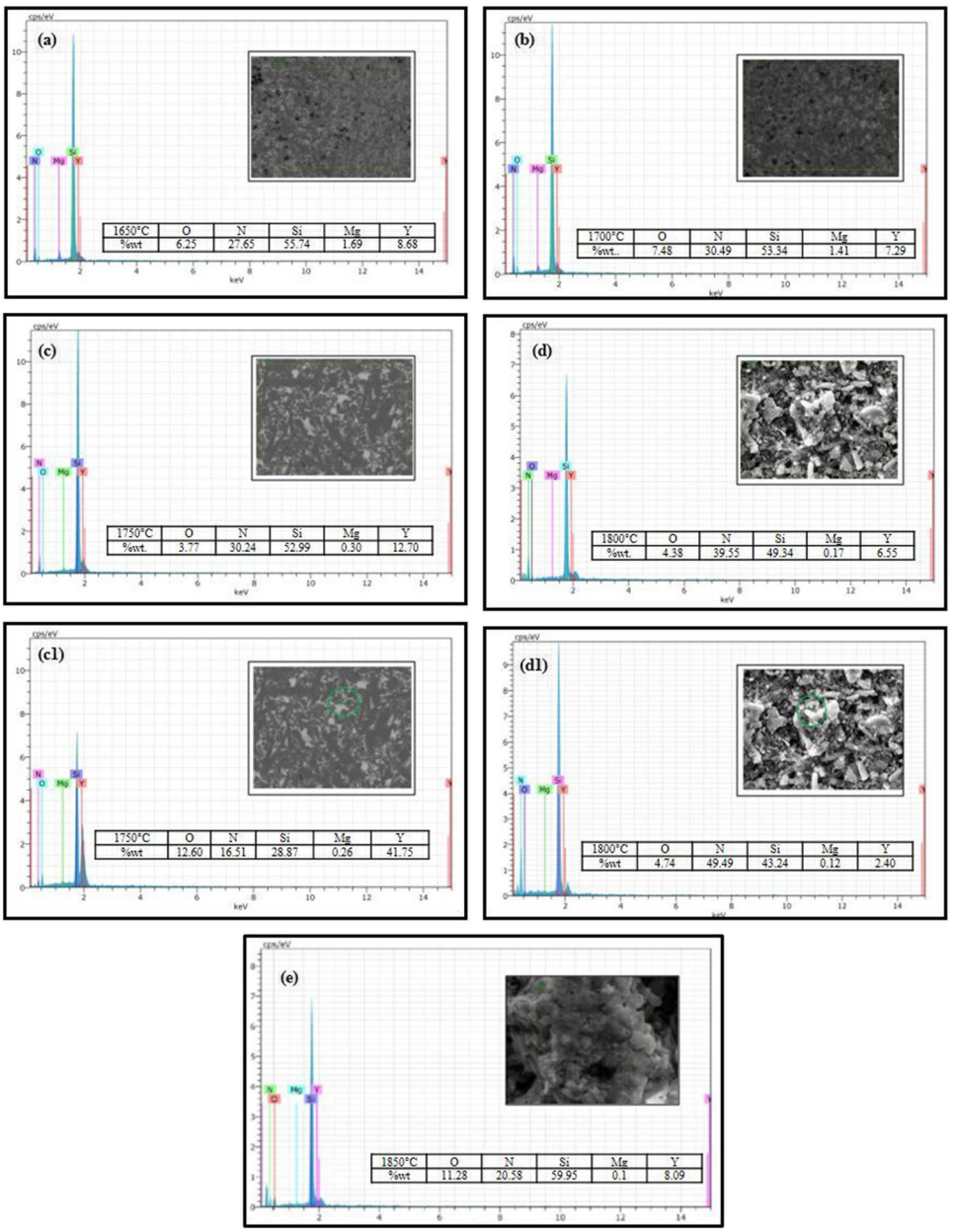

Fig. 5 EDX spectrum (field analysis) of samples sintered at temperatures of (**a**) 1650 °C, (**b**) 1700 °C, (**c**) 1750 °C, (**d**) 1800 °C, (**e**) 1850 °C, and EDX point analysis of samples sintered at temperatures of (**c1**) 1750 °C and (**d1**) 1800 °C

phase reacted with Si3N4 or N (g) in order to form gaseous SiO that was released slowly.

At higher sintering temperatures (1750 °C, 1800 °C, and 1850 °C), a very small amount of Mg was detected in the samples according to EDX results. In the samples sintered at 1750, 1800, and 1850 °C, the weight loss percent was high (10.2, 10.5, 11.1%), as confirmed by the EDX results (Fig. 5), which means that evaporation of Mg from the system occurred. It can be seen that Y, Mg, and O elements were present in the form of the secondary phase, namely melilite ($Y_2Si_3O_3N_4$). N-melilites with a general formulation of $R_2Si_3O_3N_4$ (where R = yttrium or rare earth metal) occur as an intermediate phase in the process of sintering Si_3N_4-based ceramics. In particular, melilites occur as the only secondary phase in SiAlONs which in theory can produce a satisfactory microstructure since N-melilite (M(R)) has a tetragonal structure that is located in the phase compatibility regions of α -(α—β) –SiAlONs [32–35].

The formation of melilite phase could be expressed in the form of chemical reaction by the following Eq. 4 [33].

$$Y_2O_3 + Si_3N_4 = Y_2Si_3O_3N_4 \quad (4)$$

The measured thermal diffusivity and thermal conductivity values at room temperature as well as at high temperatures are presented in Fig. 6 and Table 1. For the samples sintered at 1650 °C and 1700 °C, thermal diffusivity measured at room temperature was about 14–16 mm^2/s. For the samples sintered at temperatures of 1750 °C, 1800 °C, and 1850 °C, thermal diffusivity measured at room temperature was about 22–24 mm^2/s. Thermal diffusivity values measured at 1000 °C were 3.00 mm^2/s for the sample sintered

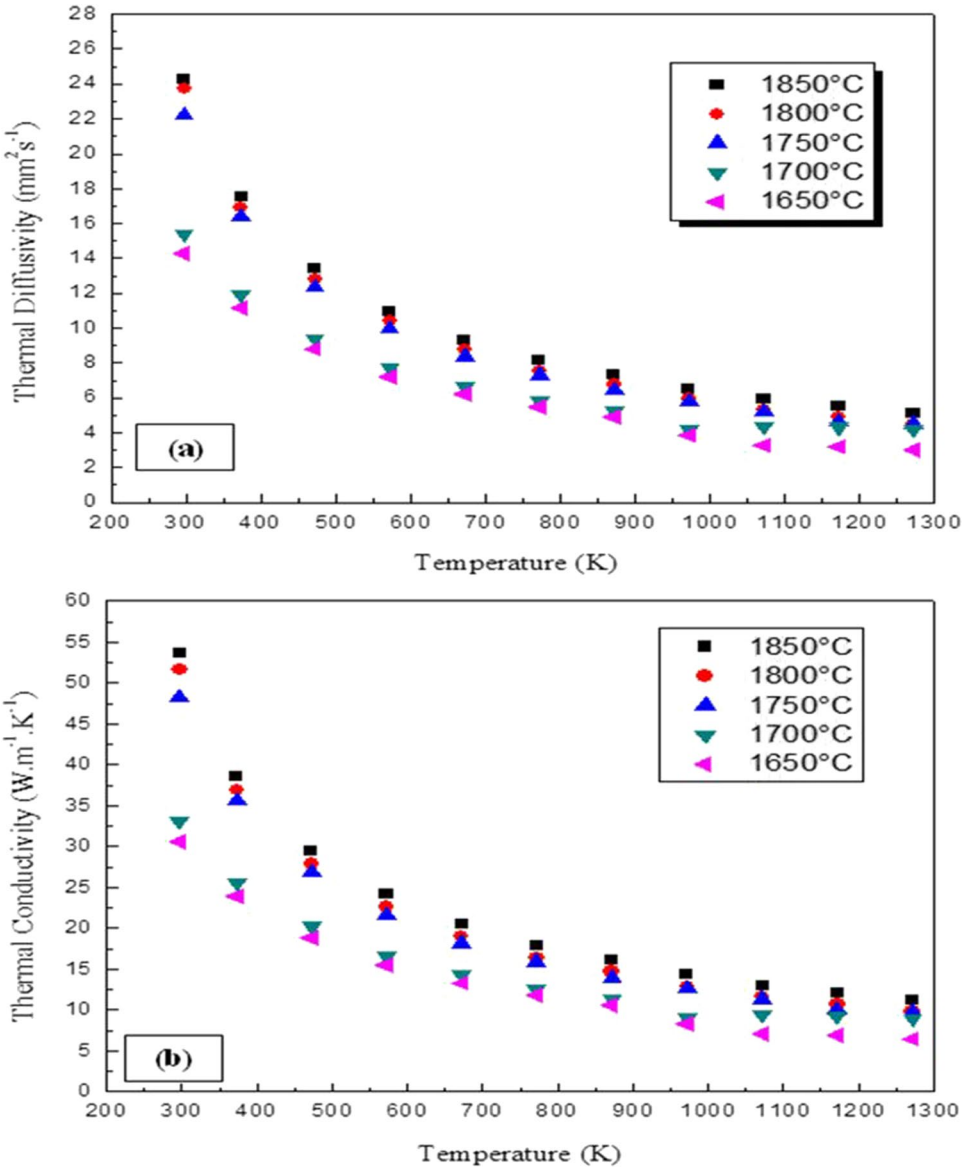

Fig. 6 (**a**) Thermal diffusivity and (**b**) thermal conductivity values of the samples as a function of measuring temperature (K)

at 1650 °C, 4.17 mm^2/s for the sample sintered at 1700 °C, about 4.50 mm^2/s for the samples sintered at 1750 °C and 1800 °C, and 5.09 mm^2/s for the sample sintered at 1850 °C temperatures (Fig. 6(a)).

The thermal conductivity value determined at room temperature was 30.53 W/(mK) and 33.05 W/(mK) for sintering at 1650 °C and 1700 °C, respectively. It was calculated as 48.26 W/(mK) for the sample sintered at 1750 °C, 51.64 W/(m.K) for the sintering temperature of 1800 °C, and 53.58 W/(mK) for the sintering temperature of 1850 °C. The thermal conductivity value determined at 1000 °C was 6.43 and 8.96 W/(mK) for sintering temperatures of 1650 °C and 1700 °C, respectively. The value was calculated as 9.77 W/(mK) for 1750 °C, 9.82 W/(mK) for 1800 °C, and 11.22 W/(mK) for 1850 °C (Fig. 6(b)). It was observed that thermal conductivity at room temperature increased with an increase in the sintering temperature and a maximum value of 53.58 W/mK was achieved in the samples sintered at temperature of 1850 °C (Fig. 6(b) and Table 1).

The comparative values of the thermal diffusivity and thermal conductivity at room temperature (25 °C) and at 1000 °C of the samples as a function of sintering temperature are given as curves in Fig. 7. The curves of the diffusivity and the conductivity values obtained at room temperature versus sintering temperature increased gradually. For the samples sintered at temperatures of 1650 °C, 1700 °C, 1750 °C, and 1800 °C, thermal diffusivity values measured at room temperature were about 14–23 mm^2/s. The highest diffusivity value measured at room temperature was 24.30 mm^2/s for the sample sintered at 1850 °C (Fig. 7(a) and Table 1). The thermal diffusivity values measured at room temperature were increased slowly with the thermal conductivity values as a function of sintering temperatures of 1650 °C and 1700 °C and above this temperature; the values were increased sharply (Fig. 7(a)).

On the other hand, for the samples sintered at temperatures of 1650 °C, 1700 °C, 1750 °C, and 1800 °C, thermal diffusivity values measured at a temperature of 1000 °C

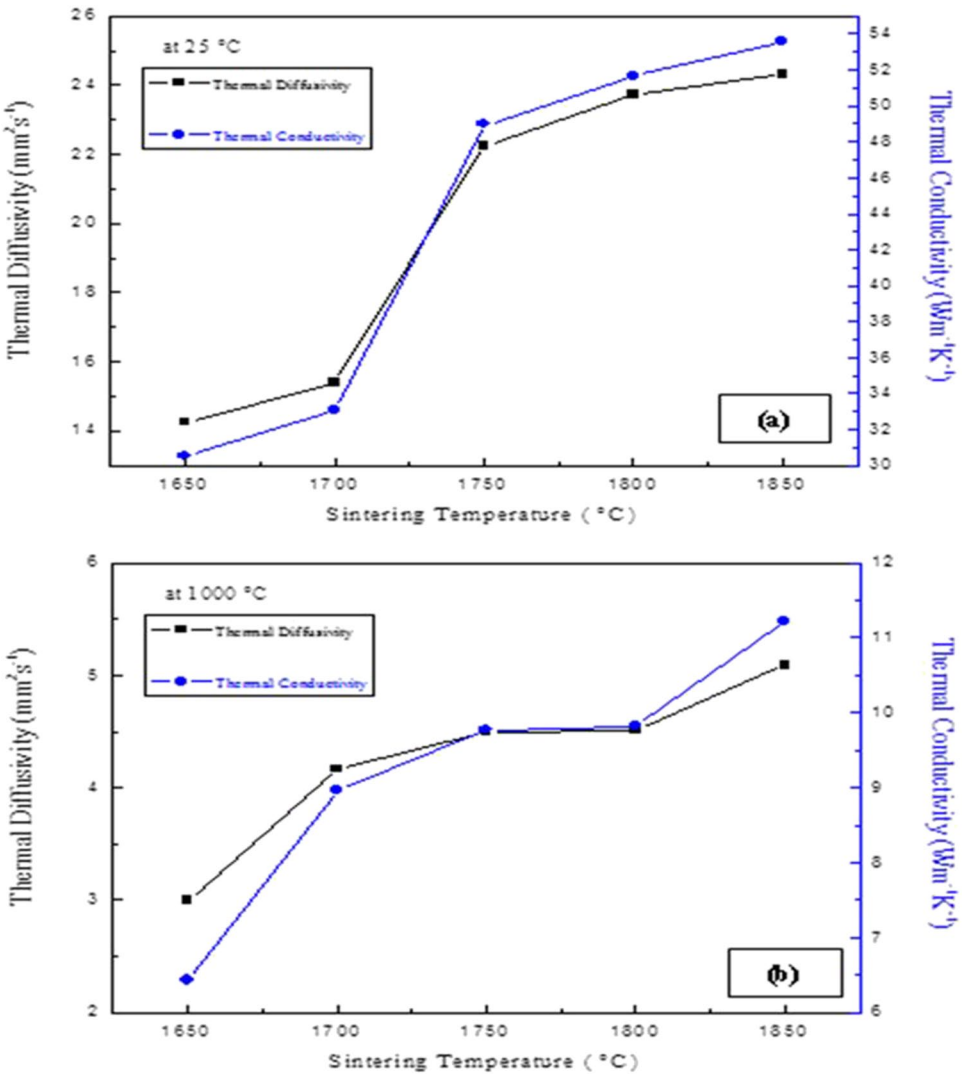

Fig. 7 Thermal diffusivity and thermal conductivity values of samples. (**a**) A room temperature and (**b**) at 1000 °C versus sintering temperature (°C)

were about 3–4.51 mm^2/s and the highest value measured as 5.09 mm^2/s for the sample sintered at 1850 °C (Fig. 7(b) and Table 1). The diffusivity values and the conductivity values obtained at 1000 °C were almost equalised as a function of sintering temperatures of 1750 °C and 1800 °C and therefore the curves levelled out followed by a slight rise (Fig. 7(b)).

The thermal conductivity and thermal diffusivity values, density, and mass change (weight loss %) values as well as consisted phases are reported in Table 1. It has already been discussed that the final properties were influenced by the formed compounds, e.g., $La_2Si_3O_3N_4$, $Y_2Si_3O_3N_4$ resulting from the reaction of Si_3N_4 and SiO_2 with the addition of rare earth oxides [34].

Thereby, it is possible to establish a relationship between crystalline phase formation and thermal properties. From the results, it can be interpreted as that the melilite ($Y_2Si_3O_3N_4$) formation affected the thermal conductivity considerably in the samples sintered at 1750 °C and above (Table 1 and Fig. 3). This is in accordance with the previous studies suggesting that the crystalline phase formation occurs in the range of 1700–1775 °C in the samples including Si_3N_4 and Y_2O_3 [34, 35]. The highest value of thermal conductivity (53.58 W/(m.K)) measured at room temperature was obtained in the samples sintered at 1850 °C. Thus, thermal conductivity increased as the sintering temperature increased; that is, an increase by about 75.5% was achieved by increasing the sintering temperature up to 1850 °C in comparison with the samples sintered at 1650 °C (Table 1).

It has been shown in the literature that the microstructure of Si_3N_4 ceramics comprised different components in the grain boundary phase and grains which are favourable to the thermal properties [16, 19, 35]. This aspect was confirmed by the samples sintered at higher temperatures which have larger particles in the microstructure, and as a consequence, the increase of the grain size caused a significant increment of thermal diffusivity (Fig. 5 and Table 1). The thermal diffusivity values of the samples were increased as a function of progressive sintering temperatures. The values obtained at room temperature were high and beyond this temperature; up to 1000 °C, reverse trend was detected possibly due to the phonon scattering process (Table 1). The total mean free path of the phonons inversely affects the scattering process at high temperature for the measurements, and hence, the phonon scattering remained low at low temperature [35].

It is necessary to point out that the phonon scattering process reduces the thermal conductivity. Therefore, it is important to reduce the phonon scattering process in order to achieve enhanced thermal conductivity. Correspondingly, the presence of crystallisation may also be considered responsible for the enhancement of thermal conductivity due to the lower phonon scattering effect [34]. Hence, in silicon nitride ceramics incorporated with the rare earth oxides, melilite ($Y_2Si_3O_3N_4$) contributes greatly to the increased thermal conductivity. It is well known that melilite phase formation occurs in the range of 1750–1850 °C [29]. It was consisted with the analyses in the samples sintered at the temperatures above 1750 °C where the presence of melilite ($Y_2Si_3O_3N_4$) was observed (Table 1 and Fig. 3). It can be attributed to the fact that with the increase of sintering temperature, crystallisation occurred despite the fact that the intensities of the melilite peaks were not significantly changed above 1800 °C (Fig. 3). It was probably due to the applied sintering process with reduced holding times to obtain cost-effective production. Besides, it was reported that the crystallisation of secondary phase is influenced by extended dwelling times during sintering and annealing process after sintering in silicon nitride ceramics [16]. In this study, the samples were not subjected to annealing treatment after sintering, and therefore, further enhancement in melilite crystallisation could not have been achieved (Table 1 and Fig. 3).

The density values and mass change values of the samples sintered in the temperature range of 1650 °C–1850 °C are presented in Table 1. The progressive increase of density with a progressive increase of mass change as a function of sintering temperature was observed. Due to comparatively low values of density being present in the samples sintered at lower temperatures up to 1750 °C, lower values in thermal diffusivity (14.25 mm^2/s, 15.38 mm^2/s) and thermal conductivity (30.53 W/(mK), 33.05 W/(mK)) were obtained. The thermal diffusivity values were increased as a consequence of the higher densities detected in the samples sintered at 1750 °C, 1800 °C, and 1850 °C. Thus, it was observed that the thermal diffusivity increased with the increasing densification.

The thermal conductivity values of the samples were increased by about 75.5% with the progressive temperature from 1650 to 1850 °C, which was following the increment of the densities of the samples probably due to the increment in grain size (Table 1 and Fig. 4). In fact, the higher the grain size, the higher the density. In previous studies, it was observed that the mean grain size directly affects the thermal conductivity considering the lattice oxygen constituent. It was noted that the larger mean grain size leads to higher thermal conductivity. Accordingly, the rare earth elements with middle ionic radius like yttria could help to increase grain size [21]. Hence, in this study, it was concluded that the thermal conductivity values of the samples were found to increase with density which was most probably due to the increasing grain size as a result of yttria, silica, and magnesia (Y_2O_3-SiO_2-MgO) incorporation.

On the other hand, it was observed that the value of mass change was increased with the increasing sintering temperature up to 1850 °C in all samples, as evidenced by EDX analyses (Fig. 5 and Table 1). The mass change could be caused by the evaporations during sintering process. Maximum

attainable values of density were achieved in almost all the samples considering high sintering temperatures. The density and open porosity values did not change significantly for the samples sintered at 1650 and 1700 °C. One interesting observation is that the open porosity values tend to increase in the temperature range of 1750–1800 °C and decreased significantly at 1850 °C with a progressive increment of density values. As a function of sintering temperature, the grain growth led to a delay in liquid filling of larger pores. This possibly resulted in the samples having coarser grains thus promotes the crystallisation in grain boundaries and causing enlarged closed pores during sintering. Hence, this supports the cause of the observed result that the density values were not directly affected by open porosity values, whereas mostly affected by existing closed pores (Table 1).

It should be noted that higher porosity reduces the intensity of thermal diffusivity as well as thermal conductivity. However, the measured thermal diffusivity and conductivity values of the samples sintered at temperatures above 1750 °C were observed to increase with increasing open porosity ratio. During sintering process, open pores transform into closed pores with increasing sintering temperature due to the densification. It may, therefore, be inferred that the thermal conductivity values were affected by not only the porosity values but also by the morphology of porosity. Meanwhile, it was detected that the porosity values were decreased rapidly for the samples sintered at 1850 °C while the density values and thermal conductivity values were increased as well. Consequently, the highest value of thermal conductivity and diffusivity was obtained in the samples sintered at 1850 °C.

[(a)]Open porosity.

[(b)]Mass change.

[(c)]Room temperature (25 °C).

Conclusions

In this study, Si_3N_4 ceramics were produced using PS at different temperatures for 2 h with SiO_2, MgO, and Y_2O_3 as sintering additives in order to obtain relatively low-cost production. In the sintering temperature effect on the microstructure and thermal properties considering these additives, the following conclusions are drawn:

A porous microstructure was observed in the sample sintered at a temperature of 1650 °C, and therefore, the lowest values of thermal diffusivity (14.25 mm^2/s) and thermal conductivity (30.53 W/(mK)) were obtained.

High temperatures above 1700 °C promoted the formation of larger particles during sintering. There was a rod-like grain development occured in the microstructure, and as the grain size increased, thermal diffusivity increased. Crystallisation is enhanced by higher sintering temperatures at the 1750–1850 °C range resulting in increasing the thermal conductivity as a result of reduced phonon scattering effect. The thermal conductivity increased by about 75.5% with the increased sintering temperature. The highest thermal conductivity (53.58 W/(m.K)) was obtained at a sintering temperature of 1850 °C.

The thermal diffusivity increased at higher sintering temperatures. While the thermal diffusivity and thermal conductivity values at room temperature vary over a wide range, this difference in these values gradually decreases with the increase in temperature and is almost equalised.

XRD results indicated that the sintering temperature had a significant effect on crystallisation. A different secondary phase ($Y_2Si_3O_3N_4$) melilite formation was detected in the samples sintered at higher temperatures led to increased density as well as enhanced microstructural properties.

Improvement of the thermal properties obtained with an addition of Y_2O_3-SiO_2-MgO could be explained by the formation of crystalline melilite phase as well as sintering temperature. The results approved that PS was an efficient method for silicon nitride ceramics in order to achieve a high performance and Y_2O_3-SiO_2-MgO to be effective sintering additives for low-cost production of Si_3N_4 ceramics that have enhanced thermal properties.

The thermal conductivity was increased in direct proportion to the density and grain size of the material. It was concluded that the higher thermal conductivity values were observed in the samples with higher weight loss due to the evaporation from the material surface.

Acknowledgements Authors would like to thank MDA Advanced Ceramics Co. (Turkey) for material support.

Author contribution Pınar Uyan: conceptualisation, characterisation, methodology, investigation, writing—original draft. Özgür Cengiz: data curation, writing—original draft, writing—review and editing. Servet Turan: conceptualisation, data curation, supervision.

Funding This study was supported by Anadolu University Scientific Research Projects under project number 1004F93 and Bilecik Şeyh Edebali University Scientific Research Foundation under project number 2016–01.BSEU.06–03.

Data availability Data could be made available on genuine request.

Declarations

Conflict of interest The authors declare no competing interests.

References

1. Lukianova, O.A., Krasilnikov, V.V., Parkhomenko, A.A.: "Microstructure and phase composition of cold isostatically pressed and pressureless sintered silicon nitride," Nanoscale. Res Lett **11**, 148 (2016)
2. Watari, K., Shinde, S.L.: High thermal conductivity materials. MRS Bull **26**, 440–444 (2001)
3. Hirao, K., Zhou, Y., Hyuga, H., Ohji, T., Kusano, D.: High thermal conductivity silicon nitride ceramics. J. Korean Ceram. Soc. **49**(4), 380–384 (2012)
4. Krüger, R., Roosen, A., Schaper, W.: Hermetic glass sealing of AlN packages for high temperature applications. J. Eur. Ceram. Soc. **19**(6–7), 1067–1070 (1999)
5. Zhou, Y., Hyuga, H., Kusano, D., Yoshizawa, Y., Hirao, K.: A tough silicon nitride ceramic with high thermal conductivity. Adv. Mater. **23**(39), 4563–4567 (2011)
6. Lee, S.: Densification, mass loss, and mechanical properties of low-temperature pressureless-sintered Si3N4 with LiYO2 additive: the effects of additive content and annealing. Int. J. Appl. Ceram. Technol. **7**(6), 881–888 (2010)
7. Yang, H., Yang, G., Yuan, R.: Pressureless sintering of silicon nitride with magnesia and ceria. Mater. Res. Bull. **33**(10), 1467–1473 (1998)
8. Parka, C., Banga, K., Parkb, D., Kimb, H., Danylukc, S.: Pressureless sintering of reaction bonded silicon nitride containing cordierite. J. Ceram. Process. Res **13**(3), 226–230 (2012)
9. Watari, K., Hirao, K., Brito, M.E., Toriyama, M., Kanzaki, S.: Hot isostatic pressing to increase thermal conductivity of Si3N4 ceramics. J. Mater. Res. **79**, 2485–2488 (1999)
10. K. Hirao, K. Watari, H. Hayashi, and M. Kitayama, "High thermal conductivity silicon nitride ceramic," MRS Bull., (2001).
11. Haggerty, J.S., Lightfoot, A.: Opportunities for enhancing the thermal conductivities of SiC and Si3N4 ceramics through improved processing. Ceramic Eng Sci Proceed, Wiley, Hoboken, NJ, USA **16**(4), 475–487 (2008)
12. Thompson, D.P.: The crystal chemistry of nitrogen ceramics. Mater. Sci. Forum **47**, 21–42 (1989)
13. Yin, S., Jiang, S., Pan, L., Liu, C., Feng, Y., Qiu, T., Yang, J.: Preparation, mechanical and thermal properties of Si3N4 ceramics by gelcasting using low–toxic DMAA gelling system and gas pressure sintering. Ceram. Int. **44**(18), 22412–22420 (2018)
14. Deeley, G.G., Herbert, J.M., Moore, N.C.: Dense silicon nitride. Powder Metall. **4**(8), 145–151 (2014)
15. Duan, Y., Zhang, J., Li, X., Bai, H., Sajgalik, P., Jiang, D.: High thermal conductivity silicon nitride ceramics prepared by pressureless sintering with ternary sintering additives. Int. J. Appl. Ceram. Technol. **16**(4), 1399–1406 (2019)
16. H. H. Lu, and J. L. Huang, "Effect of Y2O3 and Yb2O3 on the microstructure and mechanical properties of silicon nitride," Ceram. Int., (2001).
17. Ribeiro, S., Strecker, K.: Si3N4 ceramics sintered with Y2O3/SiO2 and R2O3(ss)/SiO2: a comparative study of the processing and properties. Mater. Res. **7**(3), 377–383 (2004)
18. Duan, Y., Zhang, J., Li, X., Shi, Y., Xie, J., Jiang, D.: Low temperature pressureless sintering of silicon nitride ceramics for circuit substrates in powder electronic devices. Ceram. Int. **44**(4), 4375–4380 (2018)
19. Hirao, K., Zhou, Y., Miyazaki, H., Hyuga, H.: "Improvement in thermal conductivity of silicon nitride ceramics via microstructural control and their application to heat dissipation substrates", Funtai Oyobi Fummatsu Yakin/Journal Japan Soc. Powder Powder Metall. **64**(8), 439–444 (2017)
20. Zhu, X., Zhou, Y., Hirao, K., Lenčéš, Z.: Processing and thermal conductivity of sintered reaction-bonded silicon nitride: (II) effects of magnesium compound and yttria additives. J Am Ceram. Soc **90**(6), 1684–1692 (2007)
21. Kitayama, M., Hirao, K., Kanzaki, S.: Effect of rare earth oxide additives on the phase transformation rates of Si3N4. J. Am. Ceram. Soc. **89**(8), 2612–2618 (2006)
22. Uyan, P., Turan, S.: Effect of cooling cycle after sintering on the thermal diffusivity of Y2O3 doped Si3N4 ceramics. Univers. J. Mater. Sci. **6**(1), 39–47 (2018)
23. Liao, S., Zhou, L., Jiang, C., Wang, J., Zhuang, Y., Li, S.: Thermal conductivity and mechanical properties of Si3N4 ceramics with binary fluoride sintering additives. J. Eur. Ceram. Soc. **41**(14), 6971–6982 (2021)
24. Dow, H.S., Kim, W.S., Lee, J.W.: Thermal and electrical properties of silicon nitride substrates. AIP Adv. **7**(9), 095022 (2017)
25. Kitayama, M., Hirao, K., Tsuge, A., Watari, K., Toriyama, M., Kanzaki, S.: Thermal conductivity of β-Si3N4: II, effect of lattice oxygen. J. Am. Ceram. Soc. **83**(8), 1985–1992 (2000)
26. X. Zhu, Y. Zhou, K. Hirao, T. Ishigaki, and Y. Sakka, "Potential use of only Yb2O3 in producing dense Si3N4 ceramics with high thermal conductivity by gas pressure sintering," Sci. Technol. Adv. Mater., **11**, (2010).
27. Watari, K., Seki, Y., Ishizaki, K.: "Temperature dependence of thermal coefficients for HIPped silicon nitride", Nippon Seramikkusu Kyokai Gakujutsu Ronbunshi/Journal Ceram. Soc. Japan **97**(2), 174–181 (1989)
28. Bučevac, D., Bošković, S., Matović, B.: Kinetics of the alpha-beta phase transformation in seeded Si3N4 ceramics. Sci. Sinter. **40**, 263–270 (2008)
29. Wills, R.R., Holmquist, S., Wimmer, J.M., Cunningham, J.A.: Phase relationships in the system Si3N4-Y2O3-SiO2. J. Mater. Sci. **1976**(117), 1171305–1309 (1976)
30. Langford, J.I., Wilson, A.J.C.: Scherrer after sixty years: a survey and some new results in the determination of crystallite size. J. Appl. Crystallogr. **11**, 102–113 (1978)
31. Kitayama, M., Hirao, K., Watari, K., Toriyama, M., Kanzaki, S.: Thermal conductivity of β-Si3N4: III, effect of rare-earth (RE = La, Nd, Gd, Y, Yb, and Sc) oxide additives. J. Am. Ceram. Soc. **84**(2), 353–358 (2001)
32. Ching, W.-Y.: Electronic structure and bonding of all crystalline phases in the Silica–Yttria–Silicon Nitride phase equilibrium diagram. J. Am. Ceram. Soc. **88**(7), 2011–2011 (2005)
33. Xu, W., Ning, X.S., Zhou, H.P., Lin, Y.B.: Study on the thermal conductivity and microstructure of silicon nitride used for power electronic substrate. Mater. Sci. Eng. B **99**(1–3), 475–478 (2003)
34. Lin, Y., Ning, X.S., Zhou, H., Chen, K., Peng, R., Xu, W.: Study on the thermal conductivity of silicon nitride ceramics with magnesia and yttria as sintering additives. Mater. Lett. **57**(1), 15–19 (2002)
35. Bruls, R.J., Hintzen, H.T., Metselaar, R.: A new estimation method for the ıntrinsic thermal conductivity of nonmetallic compounds: a case study for MgSiN2, AlN and β-Si_3N_4 ceramics. J. Eur. Ceram. Soc. **25**(6), 767–779 (2005)